ISSN:2320-0790

An International Journal of Advanced Computer Technology

Hyperspectral Target Detection Based on Classification Algorithms

Edisanter Lo

Susquehanna University, Selinsgrove PA 17870, USA,

loe@susqu.edu

Abstract. Target detection algorithm in hyperspectral imaging detects a certain material in a hyperspectral image using a known spectral signature of the material. Conventional algorithms for target detection assume that there is only one known target spectrum so target statistics cannot be estimated. Discriminant analysis is designed for classification, but this paper analyzes the performance of discriminant functions for target detection. The discriminant functions have been modified for target detection and uses simulated target spectra with different amount of random noise. Experimental results show that the algorithms can work well within a certain amount of noise.

Keywords: target detection, hyperspectral imaging, remote sensing

1 Introduction

Hyperspectral imaging forms images of a scene by using an imaging spectrometer to collect the reflectance spectrum of each pixel in the scene. The spectrum covers a wide range of wavelengths. Hyperspectral images have high spectral resolution and has hundreds of spectral bands. The main applications of hyperspectral imaging in remote sensing are target detection, anomaly detection, and classification. Different materials have different spectral signatures. Target detection uses a known spectral signature from an image or spectral library to detect a specific material in the image from the spectrum of the pixel. Target detection assumes the image consists of only background pixels and target pixels. Unlike classification, which requires a sample of training pixels for the background and a sample of trainng pixels for the target, target detection requires a sample of training pixels for the background and only one training pixel for the target.

The paper in [1] gives a review of target detection algorithms for hyperspectral imaging. The conventional algorithms Adaptive Matched Filter (AMF) [2] and Adaptive Coherence/Cosine Angle [3] are commonly used in target detection. A recent review of AMF and ACE is in [3]. An algorithm based on logistic regression for target detection in hyperspectral detection is in [5]. A constrained ACE detector for highly variable target is presented in [6,7].

Both AMF and ACE assume the background pixels and the target pixels form multivariate normal distributions. The AMF assumes a common population covariance Σ for both the background and target distributions. All pixels are

demeaned pixels for the AMF and ACE detectors. The AMF detector is dervied from a general likelihood ratio test and is given by

$$d(x) = \frac{s^T \hat{\Sigma}^{-1} x}{s^T \hat{\Sigma}^{-1} s}, \tag{1}$$

where the inverse of the sample covariance $\hat{\Sigma}$is $\hat{\Sigma}^{-1}$, target spectrum is s, and test pixel is x.

ACE is derived from the general likelihood ratio test. The null hypothesis tests if the distribution of the test pixel is a multivariate normal distribution with mean 0 and covariance Σ. The alternative hypothesis tests if the distribution of the test pixel is a multivariate normal distribution with mean as and covariance $\sigma^2\Sigma$. The vector s is the known target spectrum, and σ^2 and a are unknown scalars. The ACE detector for a test pixel x is given by

$$d(x) = \frac{\left(x^T \hat{\Sigma}^{-1} s\right)\left(s^T \hat{\Sigma}^{-1} s\right)\left(s^T \hat{\Sigma}^{-1} x\right)}{x^T \hat{\Sigma}^{-1} x}. \tag{2}$$

This paper proposes to modify the linear discriminant and quadratic discriminant functions for target detection and compare their performance under different noise level. Typically only one target pixel is available for training the detectors so additional training pixels for target are needed for the discriminant detectors. The target training pixels are simulated by adding a small perturbation to the mean target pixel. The source of the target spectral signature can be from the image, field measurements, or laboratory measurements. Experimental results using the mean target pixel from the image is presented in this paper.

2 Detection Algorithm

The linear discriminant and quadratic discriminant functions are classification methods that produce a binary outcome. The two discriminant functions are modified below for target detection to produce an image of detector output. The detector output is defined as the value of the modified linear discriminant or modified quadratic discriminant function.

Let the random vector X of dimensions $p \times 1$ and scalar random variable Y represent a test pixel and class, respectively. A value x of the test pixel X is to be classified as a background pixel ($Y = b$) or target pixel ($Y = t$). Let $\pi_b = P(Y = b)$, $\pi_t = P(Y = t)$, $f_b(x) = P(X = x/Y = b)$, and $f_t(x) = P(X = x/Y = t)$ denote the prior probability of a test pixel being a target pixel, prior probability of a test pixel being a background pixel, density function of X for a test pixel that is a background pixel, and density function of X for a test pixel that is a target pixel, respectively.

The Bayes' theorem states the the probability that a given test pixel is a background pixel is

$$P(Y = b/X = x) = \frac{\pi_b f_t(x)}{\pi_b f_b(x)) + \pi_t f_t(x)} \tag{3}$$

and the probability that a given test pixel is a target pixel is

$$P(Y = t/X = x) = \frac{\pi_t f_t(x)}{\pi_b f_b(x)) + \pi_t f_t(x)}. \tag{4}$$

A test pixel is classified as a target pixel if

$$\frac{\pi_t f_t(x)}{\pi_b f_b(x)) + \pi_t f_t(x)} > \frac{\pi_b f_t(x)}{\pi_b f_b(x)) + \pi_t f_t(x)}. \tag{5}$$

Assume the background pixel and target pixel come from multivariate normal distributions with mean μ_b and covriance Σ_b for the background pixel and mean μ_t and covariance Σ_t for the target pixel. The density functions for the background pixel and target pixel are given by

$$f_b(x) = \frac{1}{(2\pi)^{p/2}|\Sigma_b|^{1/2}} exp\left(-\frac{1}{2}(x-\mu_b)'\Sigma_b^{-1}(x-\mu_b)\right) \tag{6}$$

$$f_t(x) = \frac{1}{(2\pi)^{p/2}|\Sigma_t|^{1/2}} exp\left(-\frac{1}{2}(x-\mu_t)'\Sigma_t^{-1}(x-\mu_t)\right). \tag{7}$$

The linear discriminant analysis does not require the covariance of the target by assuming the background and target have a common covariance matrix, i.e. $\Sigma_b = \Sigma_t = \Sigma$. Assuming that the prior probabililies are equal, Equation (5) can written as

$$\frac{f_t(x)}{f_b(x)} > 1. \tag{8}$$

The density functions in Equation (8) can be replaced by Equation (6) and (7) to obtain the inequality

$$\frac{\frac{1}{(2\pi)^{p/2}|\Sigma|^{1/2}} exp\left(-\frac{1}{2}(x-\mu_t)'\Sigma^{-1}(x-\mu_t)\right)}{\frac{1}{(2\pi)^{p/2}|\Sigma|^{1/2}} exp\left(-\frac{1}{2}(x-\mu_b)'\Sigma^{-1}(x-\mu_b)\right)} > 1. \tag{9}$$

By combining the exponential terms and then taking natural log on both sides of the inequaity, Equation (9) can be simplified to

$$(\mu_t - \mu_b)'\Sigma^{-1}x - \frac{1}{2}(\mu_t - \mu_b)\Sigma^{-1}(\mu_t + \mu_b) \geq 0. \tag{10}$$

The detector based on linear discriminant analysis for target detection is defined as

$$d_L(x) = (\mu_t - \mu_b)'\Sigma^{-1}x. \tag{11}$$

The detector in Equation (11) is the first term from the left side of Equation (10) without the second term, which does not depend on the test pixel x. A large value of the detector would indicate a target pixel. Target detection typically

assumes target pixels are rare so the common covariance Σ can be estimated by the sample means $\hat{\mu_b}$ and $\hat{\mu}_t$ and sample covariance $\hat{\Sigma}$ computed using all pixels from the image.

The quadratic discriminant analysis assumes that the background and target have different covariance matrices, i.e. $\Sigma_b \neq \Sigma_t$. The covariance for the background can be estimated using the background pixels. There is typically only one known target pixel to be used as the target spectral signature so additional target pixels are needed to estimate the sample mean and sample covariance for the target. The additional target pixels are simulated by adding a uniform random noise to the known target pixel.

The density functions in Equation (8) can be replaced by Equation (6) and (7) to obtain the following

$$\frac{\frac{1}{(2\pi)^{p/2}|\Sigma_t|^{1/2}} exp\left(-\frac{1}{2}(x-\mu_t)'\Sigma_t^{-1}(x-\mu_t)\right)}{\frac{1}{(2\pi)^{p/2}|\Sigma_b|^{1/2}} exp\left(-\frac{1}{2}(x-\mu_b)'\Sigma_b^{-1}(x-\mu_b)\right)} > 1. \tag{12}$$

Equation (12) can be simplified to

$$-\frac{1}{2}x'(\Sigma_t^{-1}-\Sigma_b^{-1})x-(\mu_t'\Sigma_t^{-1}-\mu_b'\Sigma_b^{-1})x-k \geq 0 \tag{13}$$

where

$$k=\frac{1}{2}ln\left(\frac{|\Sigma_t|}{|\Sigma_b|}\right)+\frac{1}{2}\left(\mu_t'\Sigma_t^{-1}\mu_t-\mu_b'\Sigma_b^{-1}\mu_b\right). \tag{14}$$

The output detector based on quadratic discriminant analysis for target detection is defined as

$$d_Q(x)=-\frac{1}{2}x'(\Sigma_t^{-1}-\Sigma_b^{-1})x-(\mu_t'\Sigma_t^{-1}-\mu_b'\Sigma_b^{-1})x, \tag{15}$$

where the constant k has been dropped from Equation (12). The constant k does not depend on the test pixel x. A large value of the detector would indicate a target pixel. The means μ_b and μ_t and covariances Σ_b and Σ_t can be estimated using the corresponding sample means $\hat{\mu}_b$ and $\hat{\mu}_t$ and sample covariances $\hat{\Sigma}_b$ and $\hat{\Sigma}_t$.

3 Experimental Results

The objective of the experiment is to assess the performance of the linear discriminant analysis and quadratic discriminant analysis in target detection using a hyperspectral image from RIT (Rochester Institute of Technology). ROC curves and detector outputs are generated for the analysis. The image from RIT is shown in Figure 1. The $84 \times 146 \times 295$ image is in the visible and near-infrared wavelengths. The spatial dimensions are 84 by 146 and spectral dimension is 295. Figure 2 shows the two targets in the image, which are red felt and blue felt.

The mean target pixel used in both linear and quadratic discriminant analysis is the mean pixel from the simulated target pixels. The results presented in this section are for the red felt using the target spectra from the image. The results for the blue felt are similar to the red felt and are not shown.

The linear discriminant detector in Equation (11) requires only a sample of background pixels to estimate the common covariance, but the quadratic discriminant detector in Equation (15) requires a sample of background pixels and a sample of target pixels to estimate the covariances for the background and target. There are typically few target pixels in the image so all pixels in the image are selected as background pixels for training the detectors. Only one target pixel is assumed to be available as the target spectral signature so the mean of the target pixels from the image is used as the representative target spectral signature. A sample covariance of full rank requires at least p pixels. Both detectors use a random sample of $3 \times p$ training pixels for the target in order to obtain a good estimate of the covariance. The target training pixels are simulated using the mean target pixel from the image and a pixel of random deviates from a uniform distribution. Each pixel from the uniform distribution is scaled to have the same magnitude as the mean target pixel. Each simulated target pixel is generated by adding a scalar multiple q of the scaled pixel from the uniform distribution to the mean target pixel. The scalar q, which is a proportion of the magnitude of the target pixel, is shown in percentage in the figures.

The ROC curves for the linear discriminant detector are shown in Figure 3 for $q = 1\%, 2\%, \ldots, 10\%$. The ROC curves for the quadratic discriminant detector are shown in Figure 4 for $q = 1\%, 2\%, \ldots, 10\%$. For the range of q from 11 to 20, the ROC curves look similar to the one at $q = 10$ and are not presented here. Both the linear and quadratic discriminant detectors perform worse as more random noise is added to the simulated target pixels. The linear discriminant detector performs best at $q = 1\%$. The best ROC curves for the quadratic discriminant detector are at $q = 1\%, q = 2\%$, and $q = 3\%$. As more noise is introduced into the training pixels for the target, the performance of the linear discriminant detector gets progressively worse for the first three values of q but stays about the same after that. The performance of the quadratic discriminant detector stays about the same after the first four values of q. The roc curves show the quadratic discriminant detector performs better than the linear discriminant detector for $q \geq 2$.

The values of the detectors are used to create detector images for visual analysis of the performance of the detectors. The detector images for the linear and quadratic discriminant detectors at $q = 1\%$ are shown in Figure 5 and Figure 6. The detector images for the AMF and ACE detectors are shown in Figure 7 and Figure 8 for comparison with the discriminant detectors. The detector images show that the detectors based on discriminant analysis can detect the red felt, but the background is a little noisy. The AMF and ACE detectors show rather homogeneous background. The red felt shows up more clearly in the linear and quadratic discriminant detectors than in the ACE and AMF detectors. The detector images show the AMF detector performs worse than the ACE detector.

4 Conclusion

The linear discriminant and quadratic discriminant detectors can detect the red felt using simulated target spectra that are generated with different amount of random noise. This shows that it is feasible to solve the target detection problem, which typically has only one training pixel for the target by using classification algorithms, which require a sample of training pixels for the target. Different methods of generating the simulated target pixels and different conventional classification algorithms can be combined develop new detectors for target detection.

Acknowledgment The author wishes to thank the Center for Imaging Science, Rochester Institute of Technology, for providing the data.

Fig. 1: The 84x146 RIT image with 295 spectral bands

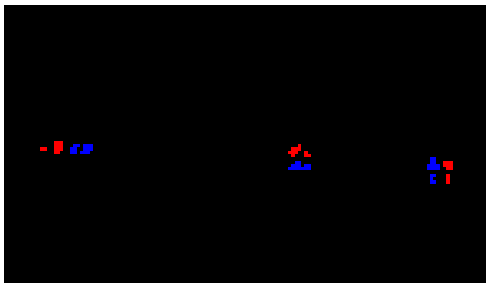

Fig. 2: The red and blue targets for the RIT image in Fig. 1.

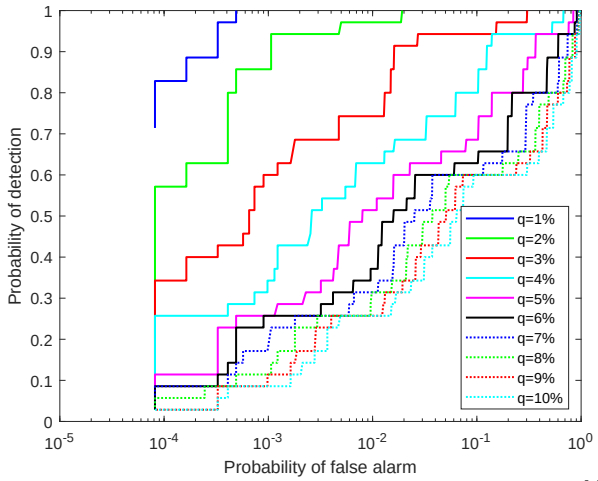

Fig. 3: ROC curves for the linear discriminant analysis for $q = 1\%$, $q = 2\%$, ..., $q = 10\%$.

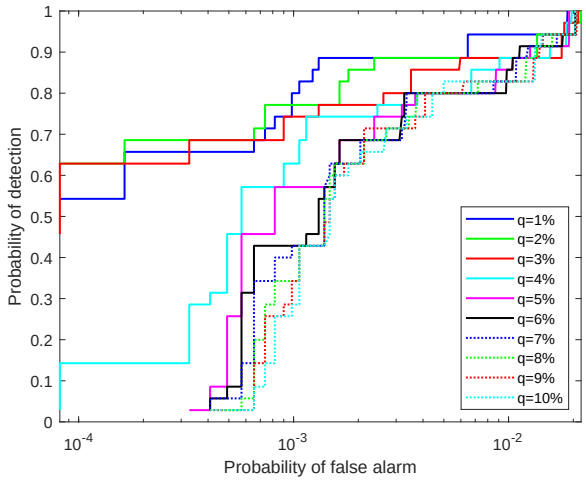

Fig. 4: ROC curves for the quadratic discriminant analysis for $q = 1\%$, $q = 2\%$,..., $q = 10\%$.

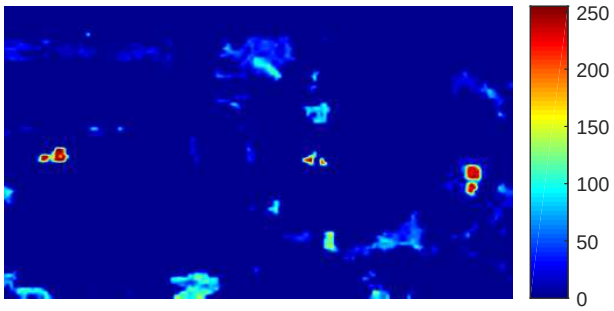

Fig. 5: Detector image for the linear discriminant detector at $q = 1\%$.

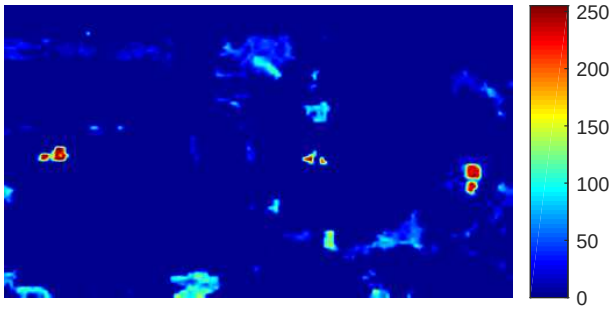

Fig. 6: Detector image for the quadratic discriminant detector at $q = 1\%$.

Fig. 7: Detector image for the AMF detector.

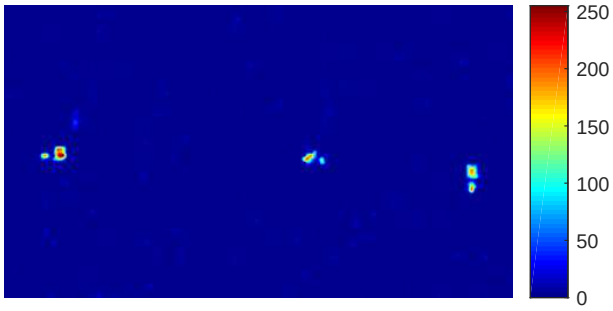

Fig. 8: Detector image for the ACE detector.

References

[1]. Manolakis, D., Shaw, G.: Detection algorithms for hyperspectral Imaging applications. IEEE Signal Processing Magazine, vol. 19, pp. 29-43 (2002).

[2]. Kraut, S., Scharf, L.: The CFAR adaptive sub-space detector is a scale-invariant GLRT. IEEE Transaction Signal Processing, vol. 47, pp. 2538-2541 (1999).

[3]. Kraut, S., Scharf, L., McWhorter, L.T.: Adaptive subspace detectors. IEEE Trans. Signal Processing, vol. 49, pp. 1-16,(2001).

[4]. Truslow, E., Manolakis, D., Pieper, M., Cooley, T., Brueggeman, M..: Performance prediction of matched filter and adaptive cosine estimator hyperspectral target detectors. IEEE Journal of Selected Topics in Applied Earth Observations and Remote Sensing, vol. 7(6), pp.2337-2349 (2014).

[5]. Lo, E., Ientilucci, I: Target detection in hyperspectral imaging using logistic regression. Proc. of SPIE, vol. 9840, 98400W (2016).

[6]. Zieman, A., Theiler, J., Ientilucci, I: Experiments with Simplex ACE:dealing with highly variable targets, Proc. of SPIE, vol. 10198, 101980F (2017).

[7]. Zieman, A., Theiler: Simplex ACE: a constrained subspace detector, Optical Engineering, vol. 56(8), 081808, pp. 1-13 (2017).